

# Discrimination between durum and common wheat kernels using near infrared hyperspectral imaging

Philippe Vermeulen<sup>a,\*</sup>, Michele Suman<sup>b</sup>, Juan Antonio Fernández Pierna<sup>a</sup>, Vincent Baeten<sup>a</sup>

<sup>a</sup> Food and Feed Quality Unit (U15), Valorisation of Agricultural Products Department (D4), Walloon Agricultural Research Centre (CRA-W), Henseval Building, Chaussée de Namur 24, 5030, Gembloux, Belgium

<sup>b</sup> Research Development & Quality, Barilla G. & R. Fratelli S.p.A, Via Mantova 166, 43100, Parma, Italy

## ARTICLE INFO

### Keywords:

Durum wheat  
Fraud detection  
Morphology  
Near infrared hyperspectral imaging

## ABSTRACT

According to Italian regulation, 3% of common wheat - CW (*Triticum aestivum*) in durum wheat - DW (*Triticum durum*) is the maximum permitted to produce pasta. Therefore, efficient methods for the detection of accidental or intentional contamination of DW products with CW are required. Until now, all the studies dealing with the detection of CW in DW have been mainly based on macroscopic, microscopic or molecular biology methods. In this recent work, near infrared (NIR) hyperspectral imaging was evaluated as a tool for discriminating between both species of wheat at the singulated kernel and bulk sample levels. This study involved the analysis of 77 samples of DW and 180 samples of CW. NIR images were acquired on a total of 4112 kernels at kernel level and on a total of approximately 51.4 kg of kernels at bulk level. To discriminate DW from CW, four approaches were studied based on morphological criteria, NIR spectral profile, protein content criteria and ratio of vitreous/non-vitreous kernels. Partial least squares discriminant analysis was used as a classification method for the construction of the discrimination models. Results showed that a combination of morphological and NIR spectral approaches could detect fraud in sample classification with 99% accuracy.

## 1. Introduction

Common wheat flour (CW - *Triticum aestivum*) is commonly used to produce bread and pastries while durum wheat semolina (DW - *Triticum durum*) is traditionally used in the production of pasta in Italy. Some Protected Designation of Origin (PDO) and Protected Geographical Indication (PGI) breads from Southern Italy require the use of durum wheat semolina in their preparation. Countries such as France, Italy and Greece regard the addition of common wheat to durum wheat in pasta production as adulteration. In some cases, mixtures of DW and CW can be attributed to a supply problem or to a significant price difference between the two species. According to current Italian regulation “Presidente della Repubblica Decreto n. 187” of 9 February 2001, possible cross-contamination with CW during the natural agricultural process cannot exceed 3% while higher percentages are considered fraudulent. Consequently, efficient methods for the detection of accidental or intentional contamination of DW products with CW are required.

Many methods have been developed in the past to detect and quantify CW adulteration in durum wheat semolina (Pasqualone,

2011). The official Italian method (Off Italian J, 1980) is based on the separation of albumins by polyacrylamide gel electrophoresis. Other discrimination methods are based on water soluble proteins using acidic capillary electrophoresis (Piergiovanni, 2007); gamma/beta gliadin detection using Reverse-phase High performance liquid chromatography (RP-HPLC) (Barnwell et al., 1994); gluten peptides using LC/ESI-MS (Prandi et al., 2012); specific protein content using UPLC-ESI-MS/MS (Russo et al., 2014); specific lipid content using HPLC (Knödler et al., 2010); and DNA sequencing using a polymerase chain reaction (PCR) (Pasqualone, 2011). All these methods are confirmatory and generally applied to semolina or bakery end-products.

However, there have been very few studies concerning the detection of CW kernels in DW kernels and until now these have been mainly based on macroscopic, microscopic or molecular biology methods. The macroscopic and microscopic morphological features of durum wheat are important criteria to discriminate among wheat species. Jayas et al. (2016), have shown the possibility of discriminating between DW and CW kernels by analyzing morphological criteria from RGB images. Molecular biology methods developed to be applied to semolina can also be applied at the kernel level although kernels contain a high

\* Corresponding author.

E-mail addresses: [p.vermeulen@cra.wallonie.be](mailto:p.vermeulen@cra.wallonie.be), [FoodFeedQuality@cra.wallonie.be](mailto:FoodFeedQuality@cra.wallonie.be) (P. Vermeulen), [Michele.Suman@barilla.com](mailto:Michele.Suman@barilla.com) (M. Suman), [j.fernandez@cra.wallonie.be](mailto:j.fernandez@cra.wallonie.be) (J.A. Fernández Pierna), [v.baeten@cra.wallonie.be](mailto:v.baeten@cra.wallonie.be) (V. Baeten).

<https://doi.org/10.1016/j.jcs.2018.10.001>

Received 4 June 2018; Received in revised form 1 October 2018; Accepted 7 October 2018

Available online 08 October 2018

0733-5210/ © 2018 Elsevier Ltd. All rights reserved.

molecular weight DNA which is not fragmented by the constraints of industrial processes.

This paper aims to explore the use of rapid screening methods at the point of entry of a production chain to control raw material compliance. As such, near infrared (NIR) spectroscopy could be considered a potentially powerful tool for this purpose. The analysis is simple, fast and non-destructive, and therefore suitable for on-line measurements. This technique is often used for authentication and traceability of agricultural and food products (Vermeulen et al., 2010, 2017; Cozzolino, 2016). Several studies have applied this technique to determine quality parameters such as protein content from the durum wheat semolina or directly from the kernels, making additional grinding or milling operations unnecessary (Sinelli et al., 2011), despite the fact that the protein content of durum wheat is generally higher than that of common wheat (INRA et al., 2017). Another important quality parameter, vitreousness, is used by the wheat industry as an indicator of milling and cooking quality. Vitreous kernels appear translucent, whereas the non-vitreous varieties (also known as starchy or mealy kernels) are opaque. Grain vitreousness/mealiness determines both its nutritional value (protein content and composition, grain pigments) and some physical features (endosperm hardness, kernel density and colour). It is generally accepted that vitreous kernels are harder and exhibit higher protein content. According to several studies, NIR infrared spectroscopy has a great potential to assess vitreousness (Wesley et al., 2005).

NIR hyperspectral imaging has also been used to determine protein content, moisture content, oil content, vitreousness and hardness, as well as to detect sprouted, insect-damaged, and fungal-infected kernels in wheat (Baeten et al., 2009; Caporaso et al., 2018). Additionally, this technology has also been used to classify wheat kernels according to their health (sound and damaged classes) (Baeten et al., 2009), the variety or class of varieties (Vermeulen et al., 2010), their vitreousness (vitreous and not fully vitreous class) (Gorretta et al., 2006) and hardness (durum, hard and soft class) (Caporaso et al., 2018). In this paper, NIR hyperspectral imaging has been defined as a fast method for the at-line and on-line discrimination between both species of wheat at the singulated kernel and bulk sample levels according to their morphological profile, NIR spectral profile, protein content and vitreousness criteria.

## 2. Material and methods

### 2.1. Samples

To assess the possible mixture of cereals in whole kernel, 3 sets of DW samples (DW1-2014: 20 samples; DW2-2015: 32 samples; DW3-2016: 25 samples) were collected in Italy in 2014, 2015 and 2016 respectively. These samples of DW covered the variability of a typical yearly harvesting campaign in terms of quality. The trials for wheat registration in the Belgium catalog enabled the collection of four sets of CW samples (CW1-2014: 30 samples; CW2-2015: 35 samples; CW4-2016: 48 samples; CW5-2016: 42 samples) representing a large variability in terms of varieties for CW (Meza et al., 2016). A single set of CW samples (CW3-2016: 25 samples) was also collected in Italy. From each of these 257 samples, a subsample of 16 kernels was selected for kernel by kernel analysis and a subsample of 200 g was extracted for bulk analysis.

### 2.2. NIR hyperspectral imaging

The instrument used for this study is an NIR Hyperspectral Imaging System (NIR-HIS) provided with a conveyor belt (BurgerMetrics SIA, Riga, Latvia). This instrument is described in detail by Vermeulen et al. (2012). All images consist of lines (320 pixels each) acquired at 209 wavelength channels: 1100–2400 nm at 6.3 nm intervals with 32 scans by image. One NIR image and  $\pm 30$  NIR images were acquired at

kernel level (subsample of 16 kernels) and at bulk level (200 g subsample) respectively for each sample. For each image of 16 kernels, eight vitreous and eight non-vitreous kernels were analyzed. In each subgroup of vitreousness, four kernels were placed on the groove side and four on the opposite side for analysis.

### 2.3. Sample characterisation

To facilitate the construction of discriminations models between the DW and CW samples described in 2.1, kernels were classified according to several morphological criteria as well as to vitreousness and samples were classified according to their protein content.

Kernels of a single specie/crop can be classified according to eight morphological criteria (Eigenvector, 2018):

Area:  $A = \pi \cdot r^2$ ; area of kernel (pixels<sup>2</sup>)

Perimeter:  $P = 2\pi \cdot r$ ; length of kernel perimeter (pixel)

Circularity:  $C = 4\pi \cdot A / P^2$ ; perfect circle:  $C = 1$

MaxFeret = Feret's diameter of kernel (length in pixels) = the longest distance between any two points along the particle boundary

MinFeret = Minimum Feret's diameter of particle (length in pixels)

AR (aspect ratio) = major\_axis/minor\_axis

Round (roundness) =  $4 \cdot \text{area} / (\pi \cdot \text{major\_axis}^2)$

Solidity = area/convex area

These parameters were calculated on each cluster, corresponding to a single kernel, obtained from the masks applied on the NIR-HIS images of 16 kernels per sample (see section 2.4.1).

Regarding vitreousness, eight vitreous kernels and eight non-vitreous kernels were selected within each sample based on visual observation.

In order to study the composition and variability of the samples set, all of them were initially analyzed using a FOSS XDS NIR spectrometer active in the 400–2500-nm range. Protein content was estimated using an equation constructed with historical NIR databases on unground wheat (Fernández et al., 2010). This equation was developed based on 3262 wheat samples and characterised by a coefficient of determination ( $R^2$ ) of 0.95 and a standard error of cross validation (SECV) of 0.3. The range of predicted protein content for the 5 sets (CW1 – CW5) was 10.3–12.3%, 9.3–10.7%, 10.7–15.6%, 10.9–12.8%, 10.8–12.8%, respectively. For durum wheat, the protein content was higher with a range of 12.1–15.1%, 10.3–13.8%, 13.2–17.4% for the three sets DW1, DW2 and DW3, respectively. The predicted values for the protein content were used to build PLS-DA models to discriminate samples with high protein content for milling wheat (HP: > 12%) and low protein content for feed wheat (LP: < 12%) (Meza et al., 2016).

### 2.4. Data treatment

Data treatment consisted of extracting the spectra relevant to kernels using a mask, to build spectral libraries of DW and CW, and develop classification models according to morphological criteria, NIR spectral profile, protein content and level of vitreousness. The entire treatment was conducted using the Matlab R2007b (The Mathworks Inc., Natick, MA, USA) and the PLS toolbox 7.0.2. (Eigenvector Research Inc., Wenatchee, WA, USA).

#### 2.4.1. Preliminary data treatment: mask, libraries

Data treatment involved building spectral libraries from images of 16 kernels for each species, i.e., DW and CW. To extract data from the image, a mask was built to isolate the kernels by applying a Partial

Least Squares Discriminant Analysis (PLS-DA) model (Barker and Rayens, 2003) combined with the density-based spatial clustering of applications with noise method (DBSCAN) (Daszykowski et al., 2001) procedure on each image. The PLS-DA model discriminates between the pixels detected as background (conveyor belt) and the pixels detected as kernels (DW or CW) based on their spectral profile. The DBSCAN is applied to account for the density of the pixels detected as kernel by the PLS-DA model. From the pre-treated images (image after applying a mask on the NIR-HIS images of 16 kernels per sample), spectral libraries for DW and CW were compiled by selecting spectra at pixel level or by calculating mean spectra on 1 or 16 kernels. The spectral libraries of pixels were used for the vitreousness criteria approach, the spectral libraries of kernels (mean of  $\pm 200$  pixels) were used for the NIR profile criterion approach, while the spectral libraries of kernel sub-samples (mean of  $\pm 200$  pixels of 16 kernels) were used for the protein content criterion approach. From these pre-treated images, spatial information of each kernel was also collected to calculate the geometric features of each kernel used on the morphological criterion approach.

#### 2.4.2. Building of classification models for DW and CW

PLS-DA was selected as the method of classification. Data treatment was performed according to four approaches: morphological criteria (C1), NIR spectral profile (C2), protein content criteria ( $< 12\%$  or  $> 12\%$ ) (C3), and vitreousness criteria (C4). The discrimination models between DW and CW were developed based on the 82 samples included in the DW1, DW2 and CW1 sample sets. Table 1 summarises the parameters (preprocessing, number of latent variables (LV), cross-validation method, calibration and internal validation sets) used to build the models as well as the performance of these models for calibration, cross-validation and internal validation according to the four approaches. This performance is expressed in terms of sensitivity, specificity and classification error, where sensitivity refers to the percentage of samples drawn from the class studied that were correctly classified by the corresponding model, and specificity refers to the percentage of samples not drawn from the class studied that were correctly classified by the corresponding model. Classification error is calculated on the basis of the sum of false positive results (100 - sensitivity) and false negative results (100 - specificity), divided by two.

The morphological approach is based on the possibility of discriminating between DW and CW by analyzing morphological criteria

from RGB images (Jayas et al., 2016). The idea is to analyze these criteria on NIR-HIS images. Eight geometric features were estimated applying the matlab procedure from each cluster (kernel) obtained by applying a mask on the images. Eight kernels of each sample were selected for the calibration set and the other eight for the internal validation set. Univariate analysis was performed on each criterion individually by calculating mean and standard deviation by sample. The Eq-1 2015 model was also developed based on the eight morphological criteria of 416 kernels of DW and 240 kernels of CW. The sensitivity and the specificity of the model in internal validation were 93.3% and 92.1%, respectively.

The NIR spectral profile approach is based on the possibility of discriminating between DW and CW by classical NIR analysis on bulk samples (Williams and Sobering, 1993). The idea is to test the NIR profile combined with spatial information to be able to discriminate between DW and CW at kernel level. The mean NIR spectra for each kernel were used to develop the discrimination model. Eight kernels of each sample were selected for the calibration set and the other eight for the internal validation set. The Eq-2 2015 model was developed based on the NIR spectral profile of 416 kernels of DW and 240 kernels of CW. The sensitivity and the specificity of the model in internal validation were 97.1% and 86.3%, respectively.

The protein content criteria approach is based on the observations that protein content is often higher in DW than in CW (France Agrimer – Arvalis, 2016). This difference was confirmed by the samples of this study showing an average protein content of 13.3% for DW, and 11.4% and 12.5% for CW from Belgium and Italy respectively. The idea was to use the mean NIR spectra calculated from the NIR-HIS images to assess protein content and thus make discrimination between DW and CW possible. First, a PLS regression model was built using the protein content predicted by a FOSS XDS instrument as reference value, and the mean NIR spectra of 16 kernels for each of the 82 samples. Nineteen samples were rejected as outliers and 63 samples were selected to be used as calibration set of the discrimination model. The Eq-3 2015 model was developed based on 23 samples with high protein content ( $> 12\%$ ) and 40 samples with low protein content ( $< 12\%$ ). The sensitivity and the specificity of the model in cross-validation were 87.0% and 87.5%, respectively.

Finally, the vitreousness criterion was used. This approach is based on the possibility of discriminating between vitreous and non-vitreous

**Table 1**  
Performance of the PLS-DA models built for the four approaches.

	Morphological criteria Kernel level (K) Durum Wheat (DW) vs Common Wheat (CW)	NIR spectral profile Kernel level (K) Durum Wheat (DW) vs Common Wheat (CW)	Protein content criteria Subsample 16 K level (Ss) High protein (HP: $> 12\%$ ) vs Low protein (LP: $< 12\%$ )	Vitreousness criteria Pixel level (px) Vitreous (Vit) vs not vitreous (nVit)
	Eq-1 2015	Eq-2 2015	Eq-3 2015	Eq-4 2015
Preprocessing	Autoscale	SNV, Der 1 2 5	SNV, Der 1 2 5	Autoscale
Latent variables number	4	12	7	6
Cross-validation	Leave on out	Leave on out	Leave on out	Venetian blinds/10 splits
Calibration set	Kernels 1–4 and 9–12 of each sample in DW1-2, CW1	Kernels 1–4 and 9–12 of each sample in DW1-2, CW1	Mean of 16 Kernels 1–16 of each sample in DW1-2, CW1	Pixels of 4 1st kernels of each sample in DW1-2, CW1
Internal validation set	Kernels 5–8 and 13–16 of each sample in DW1-2, CW1	Kernels 5–8 and 13–16 of each sample in DW1-2, CW1		
<b>Calibration</b>	<b>416 K DW, 240 K CW</b>	<b>416 K DW, 240 K CW</b>	<b>23 Ss HP, 40 Ss LP</b>	<b>30408 px Vit, 33203 px nVit</b>
Sensitivity	90.1	98.8	95.7	82.6
Specificity	93.8	99.2	90.0	82.2
Classification error	8.1	1.0	7.2	17.6
<b>Cross-validation</b>	<b>416 K DW, 240 K CW</b>	<b>416 K DW, 240 K CW</b>	<b>23 Ss HP, 40 Ss LP</b>	<b>30408 px Vit, 33203 px nVit</b>
Sensitivity	89.9	97.6	87.0	82.5
Specificity	93.8	98.8	87.5	82.2
Classification error	8.2	1.8	16.2	17.6
<b>Internal validation set</b>	<b>416 K DW, 240 K CW</b>	<b>416 K DW, 240 K CW</b>		
Sensitivity	93.3	97.1		
Specificity	92.1	86.3		
Classification error	7.3	8.3		

kernels by classical NIR analysis and on the observations that the vitreous/non-vitreous kernel ratio is often higher in DW than in CW (Dowell, 2000; Konopka et al., 2015). The idea is to use NIR spectra from the NIR-HIS images to assess the vitreousness of the kernels making it possible to discriminate between DW and CW. Given that kernels can be partially vitreous and non-vitreous, NIR spectra were used to develop, pixel by pixel, a discrimination model for each kernel. Four kernels of each sample corresponding to two vitreous kernels and two non-vitreous kernels were selected for the calibration set. The Eq-4 2015 model was developed based on the NIR spectral profile of 30408 pixels of vitreous kernels and 33203 pixels of non-vitreous kernels. The sensitivity and the specificity of the model in cross-validation were 82.5% and 82.2%, respectively.

2.4.3. Validation of PLS-DA models and expression of results

The Eq-1 2015 to Eq-4 2015 models were applied to the fully independent external validation sample sets: the 2015 CW2 set and all the 2016 sets.

For the C1 and C2 approaches, results were expressed at kernel and sample level. In the case of the morphological criteria, the Eq-1 2015 model was applied at kernel level to the images of 16 kernels subsamples and a decision rule to determine the species was defined at this level, based on the circularity (univariate analysis) and on the probability of being classified as DW (multivariate analysis) on the eight geometric criteria. For the spectral profile, the Eq-2 2015 model was applied at pixel level to the images of 16 kernels subsamples and a decision rule to determine the species was defined at kernel level, based on the % of pixels predicted as DW. Figs. 1 and 2 show the results expressed at sample level as the mean of 16 kernels ± 2SD for the morphological criteria and the spectral profile respectively. Decision rules were defined by calculating half of the difference between the mean values of the predicted values on DW and CW kernels subsamples comprising the calibration set for the criterion under study.

The results yielded by the C3 and C4 approaches, were only expressed at the sample level. The Eq-3 2015 and Eq-4 2015 models were applied at pixel level to the images of the 200 g subsamples and decision rules to determine the high/low protein content and vitreousness criteria were defined at bulk level. Figs. 3 and 4 show the results expressed at sample level as a mean of 30 images ± 2SD for protein content and vitreousness criteria respectively. The decision rules were defined by calculating half of the difference between the mean values of the predicted values on DW and CW for the 200 g subsamples

comprising the calibration set for the criterion under study.

Table 2 summarises for each approach, the decision rules and the classification results in calibration and validation at kernel and sample levels.

2.4.4. Data fusion

Data fusion consists of combining the predicted value obtained by each approach individually developed in 2.4.2, and calculating a new indicator (Di Anibal et al., 2011).

For images acquired on the 16 kernels subsamples, morphological and NIR spectral approaches were combined and an indicator was calculated as the average of the predicted values obtained by each approach. Results were expressed at kernel and sample levels. Decision rules were defined by calculating half of the difference between the mean values of the new indicator on DW and CW kernels subsamples comprising the calibration set for the criterion under study.

For images acquired on the 200 g subsamples, protein and vitreous criteria approaches were combined and an indicator was calculated as the average of the predicted values obtained by each approach. Results were expressed only at the sample level. The decision rules were defined by calculating half of the difference between the mean values of the new indicator on DW and CW 200 g subsamples comprising the calibration set for the criterion under study.

Finally, the four approaches were combined, and an indicator was calculated as the average of the predicted values obtained by each approach. Again, results were only expressed at the sample level. The decision rules were defined by calculating half of the difference between the mean values of the new indicator on DW and CW samples comprising the calibration set for the criterion under study.

3. Results and discussion

3.1. Based on the morphological criteria (C1)

The loadings plot of the PLS-DA Eq1-2015 model on geometric features shows that the first latent variable explains 57% of the variability, which is mainly linked to the circularity, the roundness, the aspect ratio (major axis/minor axis), the maxFeret and the perimeter. Indeed, the DW kernels are more elongated and the CW kernels, more circular, and rounder. In the full sample set of this study, the features calculated for DW and CW were 0.727 and 0.829 respectively, for circularity, 0.44 and 0.56 for roundness, 25.8 mm and 21.7 mm for the

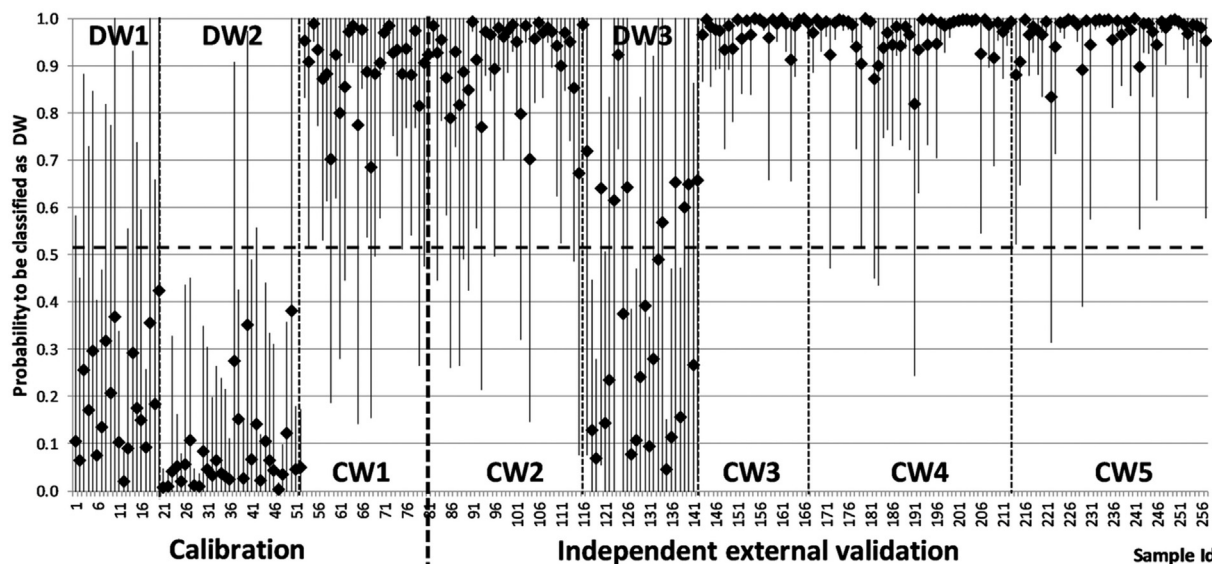


Fig. 1. Results of the morphological criteria approach applied at kernel level (C1): probability of being classified as DW (♦: mean by kernel ± 2SD) after applying the Eq-1 2015 model to the 257 images of 16 kernels.

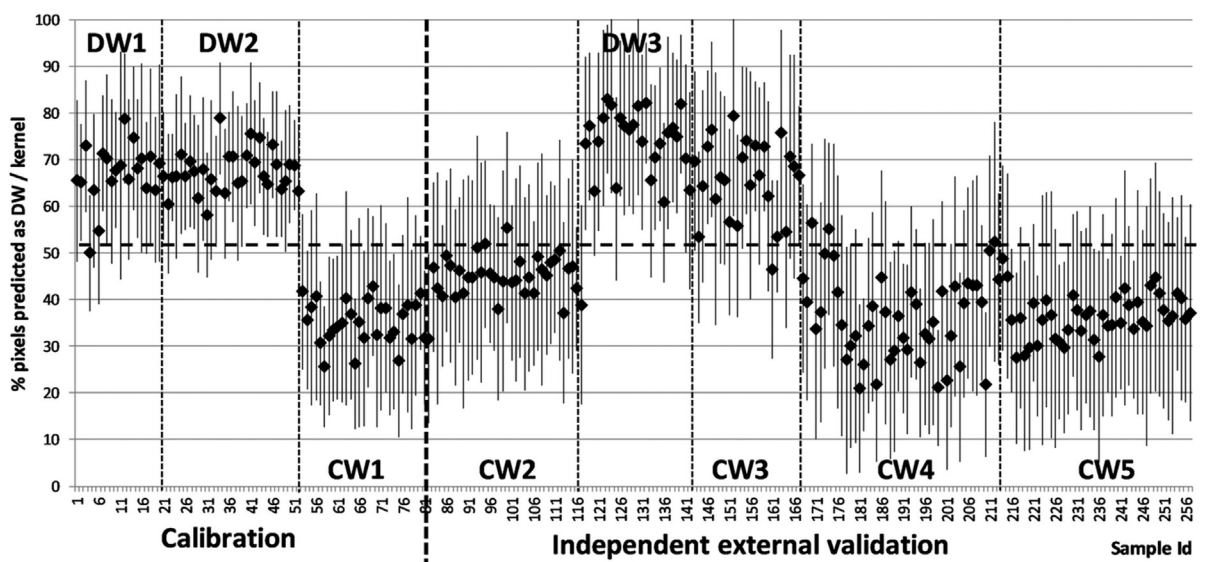


Fig. 2. Results of the NIR spectral profile approach applied at kernel level (C2): Percentage of pixels predicted as DW (♦: mean by kernel ± 2 SD) after applying the Eq-2 2015 model to the 257 images of 16 kernels.

maxFeret, 2.27 and 1.80 for the aspect ratio and, 61.9 mm and 54.7 mm for the perimeter. In Table 2, univariate analysis results for circularity at kernel and sample levels are presented in comparison to a multivariate analysis performed on the eight geometric features.

Regarding univariate analysis of the circularity criterion, a kernel or a subsample of 16 kernels is considered as belonging to the DW class if its circularity is lower than 0.767. In terms of validation, at kernel level, 71.5% of DW kernels are sorted in the cereal batch and 95.6% of CW kernels are sorted out of the cereal batch. At sample level, 76.0% of DW samples are classified as DW class and 100% of CW samples are classified as CW class and can be sorted out of the cereal batch.

For multivariate analysis, the PLS-DA Eq-1 2015 model and the threshold calculated at 0.512 were used for discriminating DW and CW. In terms of validation, at kernel level, 65.5% of DW kernels are sorted in the cereal batch and 97.4% of CW kernels are sorted out of the cereal batch. At sample level, 64.0% of DW samples are classified in the DW class and 100% of CW samples are classified in the CW class and can be

sorted out of the cereal batch. This low sorting performance for the validation set of durum wheat samples can be explained by the different varieties and pedoclimatic conditions prevailing in Italy between 2014/2015 and 2016. As the DW samples collected in 2016 were characterised by a higher circularity (0.741 mm), the equation and decision rule should be updated to account for this variability. For each image of 16 kernels per sample, Fig. 1 shows the statistic values (mean ± 2 SD) of the probability of being classified as DW after applying the PLS-DA Eq-1 2015 model. Table 2 summarises the number and percentage of CW and DW kernels/samples respectively correctly classified as compared to the other approaches.

### 3.2. Based on the NIR spectral profile (C2)

The loadings plot of the PLS-DA Eq2-2015 model on NIR spectra shows that the first latent variable explains 92% of the variability, which is mainly linked to water (1420 and 1910 nm), fat (1700 and

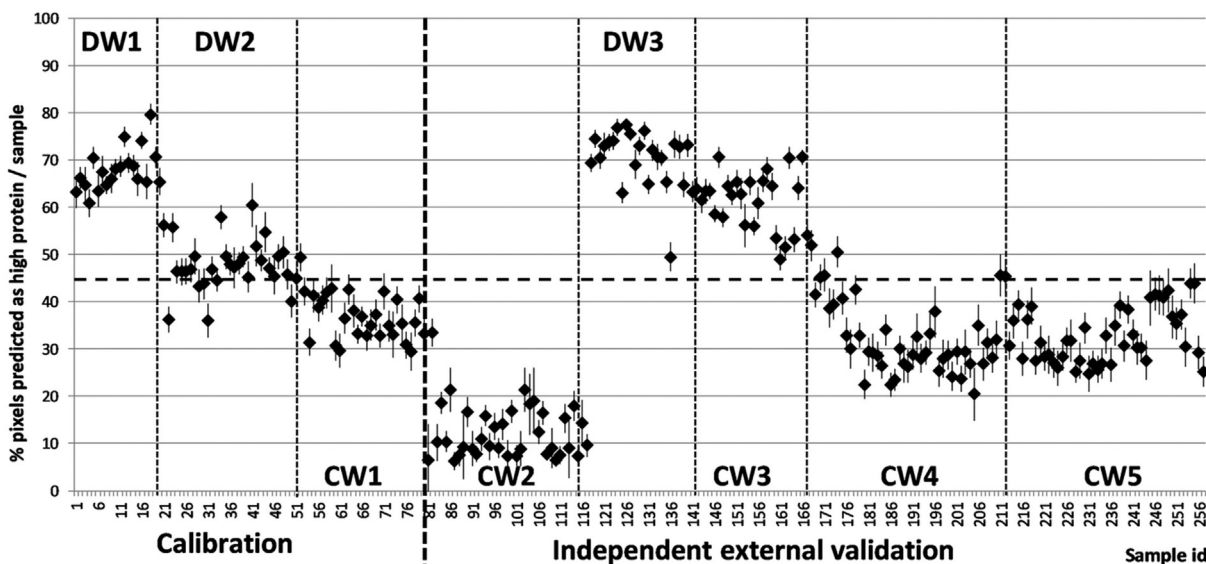


Fig. 3. Results of protein content approach applied at sample level (C3): Percentage of pixels predicted as high protein (♦: mean by image ± 2 SD) after applying the Eq-3 2015 model on the 257 samples of ± 30 images (4000 kernels).

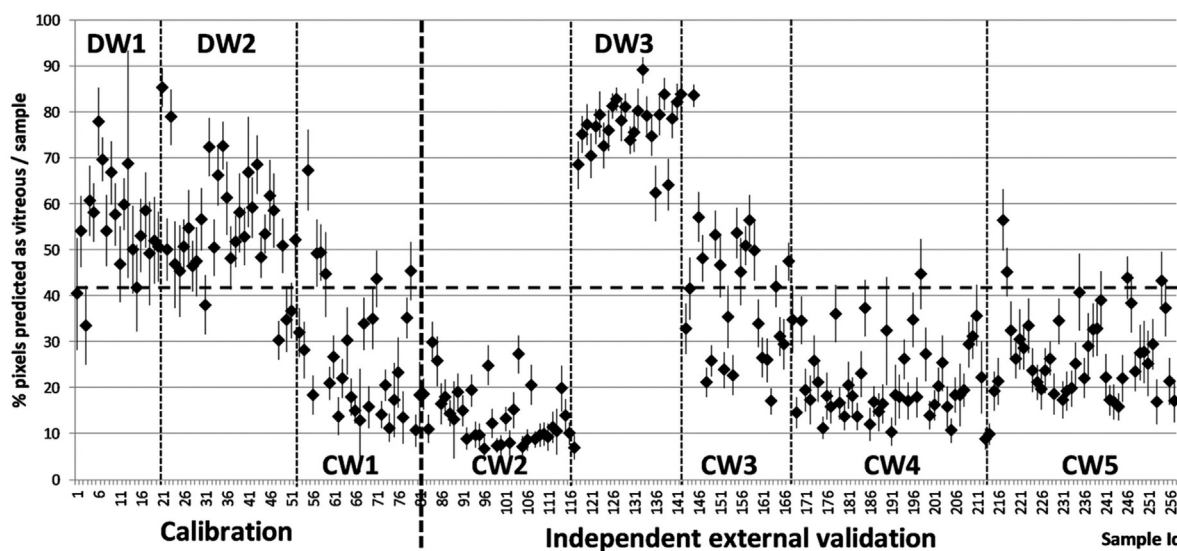


Fig. 4. Results of the vitreousness approach applied at sample level (C4): Percentage of pixels predicted as vitreous (♦: mean by image  $\pm$  2 SD) after applying the Eq-4 2015 model on the 257 samples of  $\pm$  30 images (4000 kernels).

2270 nm) and protein (2148 and 2200 nm) content. Indeed, the values predicted by NIR spectroscopy show lower water content and higher protein content in DW samples. The mean DW and CW values calculated for the whole sample set were 12.4% and 13.6% for moisture and, 13.3% and 11.6% for protein content, respectively.

The PLS-DA Eq-2 2015 model and the threshold calculated at 51.2% of pixels were used for discriminating between DW and CW. In validation, at kernel level, 97.8% of DW kernels are sorted in the cereal batch and 71.5% of CW kernels are sorted out of the cereal batch. At sample level, 100% of DW samples are classified in the DW class and 80.7% of CW samples are classified in the CW class and can be sorted out of the cereal batch. For each image of 16 kernels per sample, Fig. 2 shows the statistic values (mean  $\pm$  2 SD) of the percentage of pixels predicted as DW after applying the PLS-DA Eq-2 2015 model. Table 2 summarises the number and percentage of CW and DW kernels/samples correctly classified versus other approaches.

### 3.3. Based on protein content (C3)

The loadings plot of the PLS-DA Eq3-2015 model on protein content shows that the first latent variable explains 99% of the variability, which is mainly linked to water (1420 and 1910 nm), fat (1702 and 2274 nm), protein and gluten (1979, 2054 and 2199 nm) content. This confirms what has been already observed when using NIR spectra (2nd approach).

The PLS-DA Eq-3 2015 model and the threshold calculated at 45.5% of pixels were used for discriminating samples with low (LP: < 12%) and high (HP: > 12%) protein content. In validation, at sample level, 100% of the DW samples were classified in the HP class and 80.7% of the CW samples in the LP class and could be sorted out of the cereal batch. Amongst the CW, 97.4% and 0% of the samples from Belgium and Italy respectively can be sorted out of the cereal batch according to low/high protein content. This low sorting performance for Italian common wheat samples can be explained by the different varieties and pedoclimatic conditions prevalent in each country. The equation and the decision rule should be updated to account for this variability. For each sample of  $\pm$  30 images per sample, Fig. 3 shows the statistic values (mean  $\pm$  2 SD) of the percentage of pixels predicted as HP after applying the PLS-DA Eq-3 2015 model. A very small SD calculated on the 30 images of each sample can be observed which means that the analysis of one image corresponding to  $\pm$  7 g or  $\pm$  150 kernels could lead to the same classification. Table 2 summarises the number and

percentage of CW and DW samples correctly classified versus other approaches.

### 3.4. Based on the vitreous/non-vitreous kernel ratio (C4)

The loadings plot of the PLS-DA Eq4-2015 model on vitreousness shows that the first latent variable explains 86% of the variability, which is mainly linked to water (1420 and 1947 nm), fat (1677 and 2330 nm), protein and gluten (1476, 2023 and 2230 nm) and starch (2117 nm) content. This confirms what has been already observed using NIR spectra (2nd approach). Indeed, several studies show that protein content in vitreous kernels is higher than in non-vitreous kernels (Konopka et al., 2015).

The PLS-DA Eq-4 2015 model and the threshold calculated at 40.9% of pixels were used for discriminating between vitreous (Vit) and non-vitreous (nVit) kernels. In terms of validation, at sample level, 100% of DW samples were classified in the Vit class and 88.0% of CW samples in the nVit class and could be sorted out of the cereal batch. Amongst the CW, 92.9% and 48.0% of samples originating from Belgium and Italy respectively could be sorted out of the cereal batch according to their vitreousness. This low sorting performance for Italian common wheat samples can also be explained by the different varieties and pedoclimatic conditions of these countries. The equation and the decision rule should be updated to account for this variability. For each sample of  $\pm$  30 images per sample, Fig. 4 shows the statistic values (mean  $\pm$  2 SD) of the percentage of pixels predicted as Vit after applying the PLS-DA Eq-4 2015 model. We can also observe a very small SD calculated on the 30 images of each sample, which means that the analysis of one image could lead to the same classification, as it was the case for the approach based on protein content. Table 2 summarises the number and percentage of CW and DW samples correctly classified versus other approaches.

### 3.5. Data fusion

Data fusion techniques at kernel and sample level have been applied to all previous results (see section 3.1 to 3.4) to improve DW/CW discrimination performance by combining two or four approaches.

The left part of Table 2 shows the percentage of CW and DW kernels correctly classified according to the number of criteria used. Based on kernel by kernel discrimination, the morphological criteria and the NIR spectral profile approaches (C1 and C2) show a sensitivity of 65.5% and

**Table 2**  
Percentage of CW and DW kernels for samples correctly classified according to the number of criteria used in calibration and validation.

	Decision rule	set on 4112 kernels						on 257 samples					
		DW (1232 kernels)			CW (2880 kernels)			DW (77 samples)			CW (180 samples)		
		nb	%		nb	%		nb	%		nb	%	
<b>Univariate</b> <b>1 criterion</b> Circularity	C0 (16 kernels) DW if circularity < 0,767	cal	746/832	89.7	437/480	91.0	9.7	52/52	100	30/30	100	0	97.7
		val	286/400	71.5	2294/2400	95.6	16.5	19/25	76.0	150/150	100	12.0	
		all											
<b>Multivariate</b> <b>1 criterion</b> Morphological criteria (Fig. 1)	C1 (16 kernels) DW if probability < 0,512	cal	761/832	91.5	451/480	94.0	7.3	52/52	100	30/30	100	0	96.5
		val	262/400	65.5	2338/2400	97.4	18.6	16/25	64.0	150/150	100	18.0	
		all											
NIR spectral profile (Fig. 2)	C2 (16 kernels) DW if % pixels > 51,2%	cal	804/832	96.6	451/480	94.0	4.7	51/52	98.1	30/30	100	1.0	88.3
		val	391/400	97.8	1716/2400	71.5	15.4	25/25	100	121/150	80.7	9.7	
		all											
Protein content (Fig. 3)	C3 (200 g) DW if % pixels > 45.5%	cal	NA	NA	NA	NA	NA	43/52	82.7	30/30	100	8.7	85.2
		val	NA	NA	NA	NA	NA	25/25	100	121/150	80.7	9.7	
		all											
Vitreousness (Fig. 4)	C4 (200 g) DW if % pixels > 40.9%	cal	NA	NA	NA	NA	NA	46/52	88.5	24/30	80.0	15.8	88.3
		val	NA	NA	NA	NA	NA	25/25	100	132/150	88.0	6.0	
		all											
<b>2 criteria</b>	C1 + C2 (16 kernels) DW if average indicator > 50.0%	cal	787/832	94.6	465/480	96.9	4.3	52/52	100	30/30	100	0	98.8
		val	297/400	74.3	2349/2400	97.9	13.9	22/25	88.0	150/150	100	6.0	
		all											
<b>4 criteria</b>	C3 + C4 (200 g) DW if average indicator > 43.2%	cal	NA	NA	NA	NA	NA	48/52	92.3	28/30	93.3	7.2	87.9
		val	NA	NA	NA	NA	NA	25/25	100	125/150	83.3	8.3	
		all											
C1 + C2 + C3 + C4 (16 kernels or 200 g) DW if average indicator > 46.6%	cal	NA	NA	NA	NA	NA	52/52	100	30/30	100	0	97.7	
	val	NA	NA	NA	NA	NA	19/25	76.0	150/150	100	12.0		
	all												

97.8% respectively, and a specificity of 97.4% and 71.5% respectively in terms of validation. By combining these two criteria, sensitivity rises 74.3% and specificity 97.9%. At kernel level, the lower classification error is obtained by combining the two criteria: 4.3% in calibration and 13.9% in validation.

The right part of Table 2 shows the percentage of CW and DW samples correctly classified according to the number of criteria used. Based on discrimination at sample level in calibration, the best criteria to discriminate between DW and CW samples are morphological in nature, followed closely by NIR spectral profiles (C1 and C2). In terms of validation, by combining these two criteria, a correct classification of 88.0% is obtained for DW samples and of 100% for CW samples in validation. The combination of protein content and vitreousness criteria shows a sensitivity of 100% and a specificity of 83.0%. By combining the four criteria, a correct classification of 76% was obtained for DW samples and 100% for CW samples. The lower error classification at sample level is also obtained by combining the morphological and spectral criteria: 0% in calibration and 6% in validation.

#### 4. Conclusions

This study shows the potential of NIR hyperspectral imaging combined with chemometrics to sort kernels at the point of entry of the production chain according to the following criteria, namely: morphological, NIR spectra, protein content and vitreousness.

Models were developed based on samples collected in 2014–2015 and validated on samples collected in 2015–2016. In total, 4112 kernels were analyzed at kernel level and 257 samples of  $\pm 4000$  kernels at sample level. The models were applied either to the morphological criteria or to all the individual pixels in the images of individual kernels and bulk samples.

At kernel level, on the full set of 4112 kernels, 92.7% and 81.8% of kernels were accurately classified based on the morphological criteria and the NIR spectral profile respectively. As well, through the exclusive use of the circularity criterion, 91.5% of kernels were correctly classified. By combining these two criteria, the correct classification rate reached 94.8% of kernels.

At sample level, on the full set of 257 samples, 96.5% and 88.3% of the samples are correctly classified based on the morphological criterion and the NIR spectral profile respectively. By using either the circularity criterion or a combination of the four approaches, 97.7% of samples are accurately classified. The best classification rate of the samples (98.8%) was obtained by combining morphological criterion and NIR spectral profile. From the results on the full set of samples, it can be concluded that the performance of the models based on NIR (between 81.8% and 88.3%) is lower than the multivariate and univariate models based on a morphological criterion (between 92.7 and 97.7%) to discriminate between DW and CW. One way to improve the performance of the NIR equations could consist of updating the models and decision rules based on the variability of the 2016 wheat samples.

These results showed that the method combining the morphological criteria and the NIR spectral profile allows fraud to be detected with 98.8% accuracy permitting the correct classification of subsamples as small as 16 kernels. Models based on protein content and vitreousness are less efficient at discriminating between DW and CW but can be used to sort out low protein and low vitreousness batches inside the DW class by adjusting the thresholds.

Today, low cost RGB cameras could be used to discriminate DW and CW kernels. Classical NIR spectroscopy could be also used to assess protein and vitreousness on bulk samples. This study showed the potential of the NIR hyperspectral imaging system to combine, in one measurement, spatial information to discriminate between DW and CW and, spectral information to assess the quality (moisture, protein and vitreousness) of wheat on small samples up to kernel size. It also showed the potential of data fusion to improve the classification results. The next step should consist of taking the pilot online NIR hyperspectral

imaging system done at the laboratory level to an industrial level. A previous study performed on the identification and quantification of ergot contamination in wheat showed the transferability of the protocol between two NIR hyperspectral imaging systems instruments (Vermeulen et al., 2013).

#### Acknowledgements

The project has received funding from the European Union's Seventh Framework Programme for research, technological development and demonstration under grant agreement No.613688 (FoodIntegrity). The authors would like to thank Guillaume Jacquemin and the varieties assessment team at CRA-W for providing wheat samples, Sandrine Mauro, Stéphane Brichard and the NIR spectroscopy team at CRA-W for the NIR analyses, and Nicaise Kayoka at CRA-W for his technical support in NIR imaging.

#### References

- Baeten, V., Dardenne, P., Dubois, J., Lewis, E., Burger, J., Fernández Pierna, J.A., 2009. Spectroscopic imaging. In: Brown, S., Tauler, R., Walczak, R. (Eds.), *Comprehensive Chemometrics Chemical and Biochemical Data Analysis*. Elsevier, Oxford, UK, pp. 173–196.
- Barker, M., Rayens, W., 2003. Partial least squares for discrimination. *J. Chemometr.* 17 (3), 166–173.
- Barnwell, P., McCarthy, P.K., Lumley, I.D., Griffin, M., 1994. The use of reversed-phase high performance liquid chromatography to detect common wheat (*Triticum aestivum*) adulteration of durum wheat (*Triticum durum*) pasta products dried at low and high temperatures. *J. Cereal. Sci.* 20, 245–252.
- Caporaso, N., Whitworth, M.B., Fisk, I.D., 2018. Near-infrared spectroscopy and hyperspectral imaging for non-destructive quality assessment of cereal grains. *Appl. Spectrosc. Rev.* 1–21.
- Cozzolino, D., 2016. Near infrared spectroscopy and food authenticity. In: Espineira, M., Santaclara, F.J. (Eds.), *Advances in Food Traceability Techniques and Technologies: Improving Quality throughout the Food Chain*. Woodhead publishing, Cambridge, UK, pp. 119–136.
- Daszykowski, M., Walczak, B., Massart, D.L., 2001. Looking for natural patterns in data: Part 1. Density-based approach. *Chemometr. Intell. Lab. Syst.* 56, 83–92.
- Di Anibal, C.V., Callao, M.P., Ruisanchez, I., 2011. 1H NMR and UV-visible data fusion for determining Sudan dyes in culinary spices. *Talanta* 84, 829–833.
- Dowell, F.E., 2000. Differentiating vitreous and non-vitreous durum wheat kernels by using near-infrared spectroscopy. *Cereal Chem.* 77 (2), 155–158.
- Eigenvektor, 2018. MIA Toolbox 3.04 for Use with MATLAB TM. Eigenvektor Research Inc, Wenatchee (WA).
- Fernández Pierna, J.A., Vermeulen, P., Lecler, B., Baeten, V., Dardenne, P., 2010. Calibration transfer from dispersive instruments to handheld spectrometers. *Appl. Spectrosc.* 64 (6), 644–648.
- France Agrimer – Arvalis, 2016. Harvest 2016: Quality of French Wheat at Delivery to Inland Collection Silos. Report 12pp.
- Gorretta, N., Roger, J.M., Aubert, M., Bellon-Maurel, V., Campan, F., Roumet, P., 2006. Determining vitreousness of durum wheat kernels using near infrared hyperspectral imaging. *J. Near Infrared Spectrosc.* 14, 231–239.
- INRA, CIRAD, AFZ, FAO, 2017. Feedipedia: animal feed resources information system: wheat grains, nutritional aspects. Available on. <https://www.feedipedia.org/node/223>.
- Jayas, D.S., Paliwal, J., Erkinbaev, C., Ghosh, P.K., Karunakaran, C., 2016. Wheat quality evaluation. In: In: DA-Wen, S. (Ed.), *Computer Vision Technology for Food Quality Evaluation*, vol. 2. Academic press, London, pp. 385–412.
- Knödler, M., Most, M., Schieber, A., Carle, R., 2010. A novel approach to authenticity control of whole grain durum wheat (*Triticum durum Desf.*) flour and pasta, based on analysis of alkylresorcinol composition. *Food Chem.* 118 (1), 177–181.
- Konopka, I., Tanska, M., Konopka, S., 2015. Differences of some chemicals and physical properties of winter wheat grain of mealy and vitreous appearance. *Cereal Res. Commun.* 43 (3), 470–480.
- Meza, R., Eylenbosch, D., Monfort, B., Jacquemin, G., Bacchetta, R., Heens, B., Mahieu, O., Chavalle, S., Dumont, B., Gofflot, S., Van Remoortel, V., De Proft, M., Goffart, J.P., Sinnave, G., Bodson, B., 2016. Livre Blanc « Céréales » – Septembre 2016: 2. Variétés. Report CRA-W-GxABT™ ULG, Gembloux, pp. 155p.
- Off Italian J, 1980. Decreto ministeriale of 29 October 1979. Off Italian J 4, 3.
- Pasqualone, A., 2011. Authentication of durum wheat-based foods: classical vs. innovative methods. In: Oliveira, M.B.P.P., Mafra, I., Amaral, J.S. (Eds.), *Current Topics on Food Authentication*. Transworld Research Network, pp. 23–39.
- Piergianni, A.R., 2007. Extraction and separation of water-soluble proteins from different wheat species by acidic capillary electrophoresis. *J. Agric. Food Chem.* 55 (10), 3850–3856.
- Prandi, B., Bencivenni, M., Tedeschi, T., Marchelli, R., Dossena, A., Galaverna, G., Sforza, S., 2012. Common wheat determination in durum wheat samples through LC/MS analysis of gluten peptides. *Anal. Bioanal. Chem.* 403 (10), 2909–2914.
- Presidente della Repubblica Decreto n 187, 9 February 2001. Regolamento per la revisione della normativa sulla produzione e commercializzazione di sfarinati e paste

- alimentari, a norma dell'articolo 50 della legge 22 febbraio 1994, n. 146. *Off Italian J* 117, 6e12.
- Russo, R., Cusano, E., Perissi, A., Ferron, F., Severino, V., Parente, A., Chambery, A., 2014. Ultra-high-performance liquid chromatography tandem mass spectrometry for the detection of durum wheat contamination or adulteration. *J. Mass Spectrom.* 49 (12), 1239–1246.
- Sinelli, N., Pagani, M.A., Lucisano, M., D'Egidio, M.G., Mariotti, M., 2011. Prediction of semolina technological quality by FT-NIR spectroscopy. *J. Cereal. Sci.* 54 (2), 218–223.
- Vermeulen, P., Fernández Pierna, J.A., Abbas, O., Dardenne, P., Baeten, V., 2010. Authentication and traceability of agricultural and food products using vibrational spectroscopy. In: Li-Chan, E.C.Y., Griffiths, P.R., Chalmers, J.M. (Eds.), *Applications of Vibrational Spectroscopy in Food Science*. John Wiley & Sons, New York, USA, pp. 609–630.
- Vermeulen, P., Fernández Pierna, J.A., van Egmond, H.P., Dardenne, P., Baeten, V., 2012. On line detection and quantification of ergot bodies in cereals using near infrared hyperspectral imaging. *Food Addit. Contam.* 29 (2), 232–240.
- Vermeulen, P., Fernández Pierna, J.A., van Egmond, H.P., Zegers, J., Dardenne, P., Baeten, V., 2013. Validation and transferability study of a method based on near-infrared hyperspectral imaging for the detection and quantification of ergot bodies in cereals. *Anal. Bioanal. Chem.* 405 (24), 7765–7772.
- Vermeulen, P., Fernández Pierna, J.A., Abbas, O., Rogez, H., Davrieux, F., Baeten, V., 2017. Authentication and traceability of agricultural and food products using vibrational spectroscopy. In: Montet, D., Ray, R.C. (Eds.), *Food Traceability and Authenticity: Analytical Techniques*. Food Biology Series. CRC press, Boca Raton, USA, pp. 298–331.
- Wesley, I.J., Ruggiero, K., Osborne, B.G., Anderssen, R.S., 2005. The challenge of single estimates in near infrared calibration and prediction: the measurement of durum vitreousness using receiver instruments. *J. Near Infrared Spectrosc.* 13, 333–338.
- Williams, P.C., Sobering, D.C., 1993. Comparison of commercial near infrared transmittance and reflectance instruments for analysis of whole grains and seeds. *J. Near Infrared Spectrosc.* 1 (1), 25–32.